ACS Sustainable Chemistry & Engineering

Research Article

pubs.acs.org/journal/ascecg

Copolyesters from Soybean Oil for Use as Resorbable Biomaterials

Elayaraja Kolanthai,[†] Kishor Sarkar,[‡] Sai Rama Krishna Meka,[†] Giridhar Madras,[‡] and Kaushik Chatterjee*,[†]

[†]Department of Materials Engineering and [‡]Department of Chemical Engineering, Indian Institute of Science, C.V. Raman Road, Bangalore 560012, India

Supporting Information

ABSTRACT: A family of soybean oil (SO) based biodegradable cross-linked copolyesters sourced from renewable resources was developed for use as resorbable biomaterials. The polyesters were prepared by a melt condensation of epoxidized soybean oil polyol and sebacic acid with citric acid (CA) as a cross-linker. D-Mannitol (M) was added as an additional reactant to improve mechanical properties. Differential scanning calorimetry revealed that the polyester synthesized using only CA as the cross-linker was semicrystalline and elastomeric at physiological temperature. The polymers were hydrophobic in nature. The water wettability, elongation at break and the degradation rate of the polyesters decreased with increase in M content or curing time. Modeling of release kinetics of dyes showed a diffusion controlled mechanism underlies the observed sustained release from these polymers. The polyesters supported attachment and proliferation of human stem cells and were thus cytocompatible. Porous scaffolds induced osteogenic differentiation of the stem cells suggesting that these polymers are well suited for bone tissue engineering. Thus, this family of polyesters offers a low cost and green alternative as biocompatible, bioresobable polymers for potential use as resorbable biomaterials for tissue engineering and controlled release.

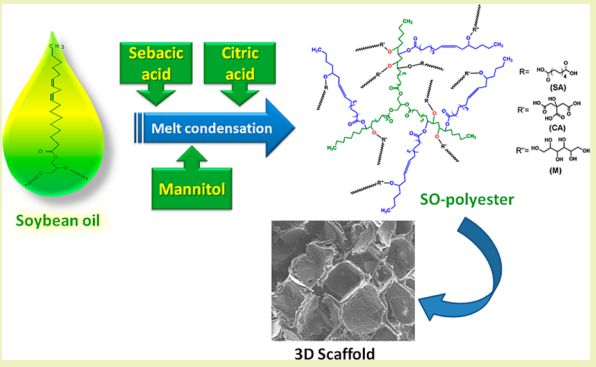

KEYWORDS: *Polyester, Elastomer, Renewable resources, Tissue scaffold, Controlled release*

INTRODUCTION

Tissue engineering is a rapidly emerging field of medicine, as it promises to treat millions worldwide suffering from loss of tissue function due to damage from injury or trauma. Successful tissue regeneration involves the use of a three-dimensional (3D) scaffold with an open porous structure and of sufficient mechanical properties to facilitate cell growth, proliferation, and differentiation for tissue formation.[1,2] The biomaterial for an ideal scaffold must be biocompatible and biodegradable to be resorbed as the tissue forms. Various types of scaffolds prepared from ceramics, naturally derived polymers and synthetic polymers have been used for tissue engineering.[3] Biodegradable polymers are useful as their degradation rate, biodegradability, processing routes and chemical functionalization can be tuned to optimize mechanical properties, control scaffold architecture and control cell response.[4−6]

Several biodegradable polymers such as polyanhydrides,[7] polyorthoesters,[8] polyphosphazenes,[9] polyhydroxyalkanoates[10] and the polyesters of polyglycolic acid (PGA),[11] polylactic acid (PLA),[12] polylactide-*co*-glycolide (PLGA),[13] polyurethane,[14] etc. have been developed for biomedical applications including drug delivery and tissue engineering. Many of these polymers are expensive, derived from nonrenewable sources and the synthesis requires toxic catalyst and/or large volumes of organic solvents.[4,15] In addition, the mechanical properties of these polymers do not mimic that of human tissues and thus are not well suited for tissue engineering. Therefore, there is a need to develop low cost biodegradable polymers for tissue engineering derived from renewable sources and prepared by green synthesis routes.

Soybean oil (SO) is one of the cheapest vegetable oils that is abundantly available. Polyurethanes prepared from SO have been reported in recent years.[16−18] In general, polyurethanes tend to exhibit slower degradation rates compared to polyesters,[19] which is leveraged for biomedical applications requiring chemically stable, nondegradable materials such as tubing, catheters, drapes, wound dressing, and in some drug delivery devices.[20] The high melting temperature of polyurethanes compared to polyesters is suggested to be a plausible mechanism underlying enhanced stability.[21] For tissue engineering, scaffold prepared from bioresorbable polyesters, which are susceptible to hydrolytic and enzymatic degradation are widely utilized. There are few reports on the synthesis of SO based polyesters.[22−24] However, SO based polyesters have not been reported for biomedical applications previously.

Triglycerides are the major component in SO and these include both saturated and unsaturated fatty acids.[25] Epoxidation followed by oxirane ring opening is the best method to

Received: January 1, 2015
Revised: March 19, 2015

DOI: 10.1021/acssuschemeng.5b00001
ACS Sustainable Chem. Eng. XXXX, XXX, XXX−XXX

prepare polyols from SO using inorganic acids, alcohols, and hydrogenation.[26] Ricinoleic acid (RA) consists of hydroxyl and carboxyl functional groups for the formation of polyols and ester linkage in the polymer backbone.[27] It is a bioactive molecule that has analgesic and anti-inflammatory uses[28] and is released when the polymer degrades. Fatty acids are disposed from the body by the β-oxidation pathway. D-Mannitol (M) is derived from mannose and is metabolized in an insulin independent manner.[29] Citric acid (CA) is a readily available, inexpensive monomer with multifunctional groups and is known to act as a cross-linker. It is reactive and forms hydrogen bonding within a polyester matrix. It is an intermediate in the Krebs or the CA cycle.[30] Sebacic acid (SA) is an easily available biocompatible monomer, used as a biopolymer and chemotherapy agent.[31] SA is completely converted into acetyl CoA and succinyl CoA that subsequently enters the Krebs cycle. Thus, all these monomers used to prepare polymers were nontoxic and can be eliminated safely from the human body after degradation.

The aim of this work was to prepare biocompatible, biodegradable copolyesters, which are elastomers from SO and SA using CA as the cross-linker. Mannitol was used as an additional reactant to improve the mechanical properties of the polymers. All these monomers are obtained from the renewable resources. In this study, we have prepared SO based copolyesters by melt condensation. The mechanical properties were tailored by varying the curing process and cross-linker concentration. Physico-chemical properties, release kinetics and human stem cell response on the polyester surface were characterized for potential use as biodegradable biomaterials.

EXPERIMENTAL SECTION

Materials. Consumer refined soybean cooking oil was procured from Fortune-Adani Wilmar, India. RA and SA were purchased from Sigma-Aldrich. All the monomers used were 99% pure. Glacial formic acid, sulfuric acid, hydrogen peroxide, and CA were purchased from Merck, India. Tetrahydrofuran (THF), dimethylformamide (DMF), and M were brought from S.D. Fine Chemicals.

Synthesis of Epoxidized SO and SO Polyol. Epoxidized SO (ESO) was synthesized according to the previous report.[32] 100 mL of SO and 11 mL of glacial formic acid were taken in a round-bottom flask placed in an oil bath at 55 °C. 0.5 mL of concentrated sulfuric acid was added to the mixture with constant stirring followed by dropwise addition of 81 mL of 30% hydrogen peroxide, and the reaction was continued for 7 h at 55 °C. The crude product was filtered to remove excess water and then washed with water several times to neutralize the product. Finally, the light yellowish colored ESO was obtained by rotary evaporation followed by vacuum drying at 60 °C.

SO polyol (SO−OH) was prepared by the ring opening reaction of ESO. For this reaction, 3 g of ESO and 1 g of RA were taken in a 100 mL three-neck round-bottom flask equipped with a reflux condenser. The reaction mixture was refluxed with continuous stirring at 160 °C for 8 h under nitrogen atmosphere. During reaction, the solution color changed from light yellow to wine red and finally to a dark red viscous liquid. The synthesized SO−OH was used directly at the subsequent stage to synthesize the SO based polyester.

Synthesis of Soybean Oil based Polyester. A family of polyesters was prepared by initially reacting up to four different components (SO−OH, SA, CA and M) to form the prepolymer and subsequently curing the prepolymer. When the prepolymer was prepared from either two or three components, as listed in Table 1, the components were taken in a 100 mL three neck round-bottom flask and mixed using a magnetic stirrer at 160 °C for 120 min with continuous nitrogen purging. When all the four components were used to prepare the polymer, the weighed amounts of SO−OH, SA and CA were taken and melted as mentioned above with constant stirring for 90 min under nitrogen purging. Subsequently, M at different weight ratios, as listed in Table 2, was added to the reaction mixture. The reaction was continued for 30 min under the same condition. After cooling, the obtained prepolymer was transferred to a Teflon Petri dish and postpolymerized at 120 °C without vacuum at 3 and 5 days to obtain the final polyester. The postpolymerized polyesters are referred to as MX wherein X indicates the content (weight ratio) of M in the polymer. The weights taken and the compositions of the different polyesters prepared in this work are listed in Table 2.

Table 1. Composition of Polymers Containing Either CA or M Cured at 120° C for 5 Days

weight (g)					
SO−OH	SA	CA	M	weight ratio SO−OH:SA:CA:M	remarks
2	1	1	0	1:0.5:0.5:0[a]	elastomeric but soft
2	1	2	0	1:0.5:1:0	brittle polymer; crumbles into powder and fragments after curing
2	2	1	0	1:1:0.5:0	
2	4	1	0	1:2:0.5:0	
2	4	2	0	1:2:1:0	
2	1	0	2	1:0.5:0:1	

[a]Same as M0 in Table 2.

Characterization. The proton (^{1}H) and carbon (^{13}C) nuclear magnetic resonance spectra of modified SO and prepolymers were recorded at 400 MHz in a Bruker NMR spectrometer. Acetone d_6 and tetramethylsilane were used as the solvent and the internal reference, respectively. Prepolymers were purified by solution precipitation method according to our previous report[33] before NMR characterization. Fourier transform infrared (FTIR) spectra of SO, ESO, SO−OH, and synthesized polyesters were recorded using PerkinElmer Spectrum 100 FTIR spectrometer attached with attenuated total reflection (ATR) accessories. Differential scanning calorimetry (DSC) thermograms were recorded using a TA Instruments Thermo DSC Q100 in the range of −50 to +250 °C at a heating rate of 10 °C/min. The melting point, glass transition, and crystallization temperature of synthesized polyesters were analyzed from DSC thermograms. The static water contact angle of all postpolymerized polyesters surface was measured by sessile drop method using Dataphysics contact angle equipment at 25 °C. The contact angle of the liquid−solid interface was determined by placing a small drop of water (1 μL) through a microsyringe on the polymer film and simultaneously recording the angle made with the tangent using SCA20 software. The measurement was carried out at three different positions on each polymer surface and averaged. The mechanical properties of all polyesters at different postpolymerization time were carried out using 10 N load cell (Mechanism micro universal testing machine) and data acquisition software. All samples were cut into dog-bone shapes using a punching machine, and the experiment was carried out at room temperature with stain rate of 5 mm/min (ASTM D638). The elastic modulus was measured from the initial slope of the stress−strain graph, and the experiment was carried out six times for each sample and averaged.

The molecular weight of polymer chain in between the cross-links and the cross-linking density were measured using the rubber elasticity equation:

$$n = \frac{E_0}{3RT} = \frac{\rho}{M_c} \quad (1)$$

In eq 1, n is number of active network chain segments per unit volume (mol/m^3); E_0 is Young's modulus (Pa), R is universal gas constant (8.314 J/mol K), T is absolute temperature (300 K), M_c is the molecular weight between the cross-links (g/mol), and ρ is the polymer density (g/m^3). The ρ of the synthesized polymers was calculated using water by Archimedes' principle.

In Vitro Degradation. To characterize the degradation in vitro, the postpolymerized polymer films (8 × 8 × 1 mm) were taken in nylon mesh bags and immersed in 20 mL of phosphate-buffered saline

DOI: 10.1021/acssuschemeng.5b00001
ACS Sustainable Chem. Eng. XXXX, XXX, XXX−XXX

Table 2. Composition, Swelling Ratio and Sol Content of Polymers Containing Both CA and M cured at 120° C

	weight (g)						swelling ratio		% of sol content	
code	SO−OH	SA	CA	M	weight ratio SO−OH:SA:CA:M	remarks (5 day cured)	3 day cured	5 day cured	3 day cured	5 day cured
M0	2	1	1	0	1:0.5:0.5:0	elastomeric but soft	3.2 ± 0.3	3.0 ± 0.3	14 ± 1	10 ± 2
M0.05	2	1	1	0.10	1:0.5:0.5:0.05	elastomeric and progressively higher elastic modulus with increasing M content	3.0 ± 0.4	2.6 ± 0.2	12 ± 1	9 ± 1
M0.15	2	1	1	0.30	1:0.5:0.5:0.15		2.9 ± 0.1	2.2 ± 0.4	11 ± 1	8 ± 1
M0.25	2	1	1	0.50	1:0.5:0.5:0.25		2.7 ± 0.2	1.9 ± 0.3	10 ± 1	7 ± 1
M0.50	2	1	1	1	1:0.5:0.5:0.5	brittle and hard	2.0 ± 0.2	1.5 ± 0.2	6 ± 1	4 ± 1

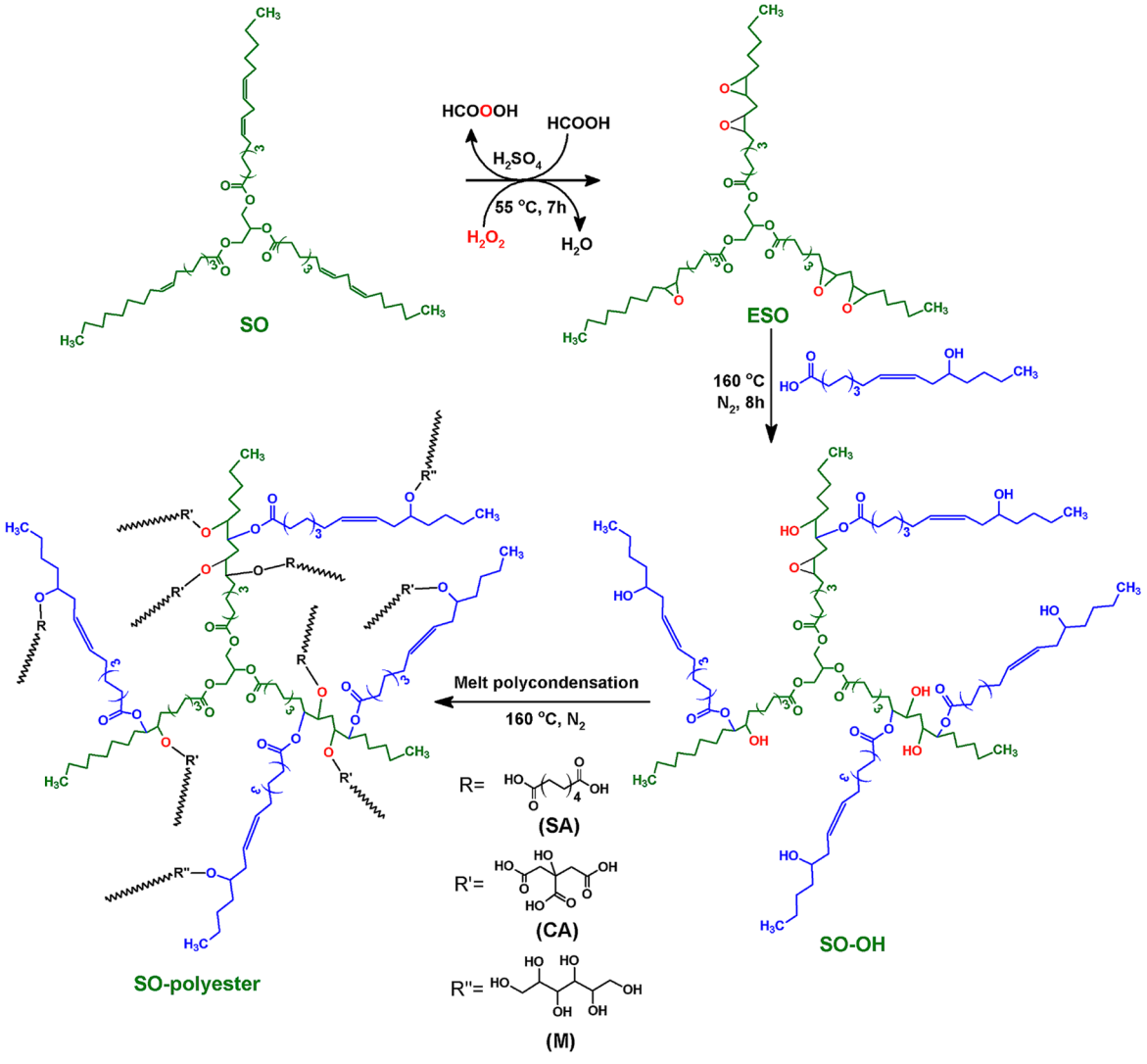

Figure 1. Schematic illustration for preparation of SO−OH and followed by SO based polyesters.

(PBS; pH 7.4) with constant shaking at 100 rpm at 37 °C. Samples were removed from PBS at predetermined time points and dried at 50 °C until constant weight was attained. The percentage mass loss of the polymer was calculated from the following equation:

$$\%M_{loss} = \frac{M_0 - M_t}{M_0} \times 100 \quad (2)$$

where M_0 is the mass of polymer before degradation and M_t is the mass of polymer after degradation at specified time t.

In Vitro Dye Release. To assess the release capability of the polyester, the release of model dyes was investigated. 10 wt % Rhodamine B (RB, hydrophilic) and Rhodamine B base (RBB, hydrophobic) dyes were dissolved in 3 mL of *N*,*N*-dimethyformamide (DMF) followed by addition of 90 wt % prepolymers (M0 and M0.25) in a Teflon Petri dish with constant stirring to make a homogeneous solution. The solvent was evaporated from the dye loaded polymer in a laminar air flow chamber at 25 °C for 2 days followed by postpolymerization at 120 °C for 3 and 5 days. The dye loaded M0 and M0.25 postpolymerized films (8 × 8 × 1 mm) were taken in a cotton bag and immersed in 20 mL of PBS (pH 7.4) at the physiological temperature of 37 °C with continuous shaking at 100 rpm for dye release study. 200 μL of the solution containing the released dye was withdrawn at definite time intervals for measurement and replaced with 200 μL of fresh PBS. The amount of dye released from the polymers was determined by measuring the absorbance (λ =

DOI: 10.1021/acssuschemeng.5b00001
ACS Sustainable Chem. Eng. XXXX, XXX, XXX−XXX

553 nm) using a microplate reader (BioTek Synergy HT). All experiments were carried out in triplicate.

Fabrication and Characterization of Films and Porous Scaffolds. 30 wt % M0 and M0.25 prepolymers were dissolved in tetrahydrofuran (THF) and used for preparation of flat films (two-dimensional, 2D) and macroporous 3D scaffolds. For films, 100 μL polymer solutions were drop casted on microscope coverslips (12 mm diameter) and subsequently dried at room temperature. 3D porous scaffolds of M0.25 with dimensions of 8 mm diameter and 3 mm height were fabricated by a salt leaching method. 0.5 mL of polymer solution was added to a 2 mL polypropylene centrifuge tube containing 2 g of NaCl crystals sieved to a size range of 250−425 μm. The tube was centrifuged at 1.3×10^4 rpm for 20 min to facilitate the ingress of the polymer solution into the packed NaCl bed, and subsequently air-dried overnight to remove the solvent. The films and the scaffolds were kept in an oven at 120 °C for 5 days for postpolymerization. After the polymer cured, the tube containing the scaffolds was cut into 3 mm height. The salt particulates were leached out in deionized water for 5 days with repeated changes of the water every 12 h. Finally, the scaffold was freeze-dried (Labconco) for 1 day. The surface morphology and pore size of the scaffold were analyzed using scanning electron microscopy (SEM, FEI ESEM Quanta 200).

Stem Cell Studies. Bone marrow derived human mesenchymal stem cells (hMSCs, Stempeutics) from a 25 year old male donor were cultured in growth medium (GM) composed of knockout Dulbecco's modified Eagle's media (KO DMEM, Invitrogen) supplemented with 15% MSC-qualified fetal bovine serum (Invitrogen), 1% glutamax, and 1% antibiotic mixture of penicillin−streptomycin (Invitrogen), and incubated at 37 °C in a humidified atmosphere with 5% CO_2. Passage 4 cells were used for all studies reported herein.

Prior to cell seeding, films and scaffolds were washed in ethanol and dried under UV light. Films of M0 and M0.25 were placed in 24-well plates and 1×10^4 cells were added to each well. Porous scaffolds were inserted in 48-well plates and were seeded with 1×10^4 cells for each well. Cells grown on the tissue culture polystyrene (TCPS) well surfaces were taken as the controls. hMSC viability on films and scaffolds was evaluated using WST-1 assay (water-soluble tetrazolium salts, Roche) at 1, 3, and 7 days. At each time interval, culture medium was removed and samples were washed with PBS. 400 μL of 10% medium containing WST-1 was added to each well and incubated for 3 h to observe the color change from pink to yellow. Optical absorbance was measured at 440 nm using a microplate reader. To observe cell morphology, samples were fixed with 3.7% formaldehyde, dried, sputter coated with gold, and observed under SEM.

Osteogenesis and mineralization in vitro was studied using Alizarin red S (ARS) dye on 3D scaffolds cultured with hMSCs for 7 and 14 days in GM. Cells grown on TCPS in GM and osteogenic medium (OM) containing known osteogenic supplements, as reported previously, were taken as the controls.[34] At each time point, cells were fixed with 3.7% formaldehyde for 30 min and stained with 2% AR dye for 20 min and washed several times with deionized water to remove excess stain. The stain was dissolved in 0.5 mL of 0.5 N HCL containing 5% SDS for 30 min. The absorbance of the dissolved AR stain was measured at 415 nm using a microplate reader and quantified. Separately, the mineral deposition on scaffolds was analyzed using SEM with energy dispersive X-ray analysis (SEM-EDX).

Statistical Analysis. Statistical analysis of WST and AR assay data (six replicates each) was carried out by one-way analysis of variance (ANOVA), and differences were considered statistically significant for $p \leq 0.05$.

RESULTS AND DISCUSSION

Polyester Synthesis. A family of SO based polyesters was synthesized by solvent and catalyst free melt polycondensation of SO−OH with other monomers derived from renewable resources such as SA, CA, and M. First, SO−OH was synthesized by epoxidation of SO followed by ring opening reaction of ESO by RA (Figure 1). The synthesized ESO and

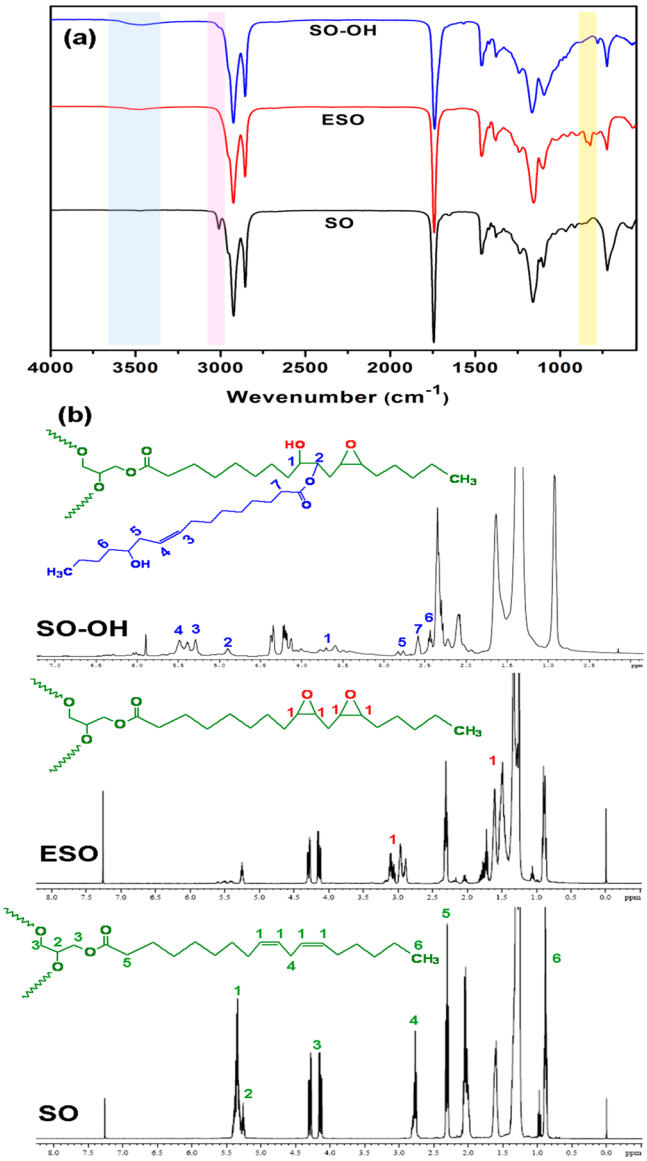

Figure 2. Chemical characterization of chemically modified SO. FTIR spectra of SO, ESO, and SO−OH (a), and ^{1}H NMR spectra of SO, ESO, and SO−OH (b).

SO−OH were characterized by FTIR spectroscopy, as shown in Figure 2a. The IR spectra of the SO show the following characteristic absorption peaks: 3013 cm^{-1} (trans = C—H stretch), 2922, and 2852 cm^{-1} (asymmetric and symmetric stretching of $-CH_2$, respectively) and 1744 cm^{-1} (C═O stretching of triglyceride).

The intensity of the peak at 3013 cm^{-1} corresponding to the double bonds presented in SO was much lower compared to that of $-CH_2$ stretching (2922 and 2852 cm^{-1}) and C═O stretching (1744 cm^{-1}). After epoxidation, the peak at 3013 cm^{-1} completely disappeared and a new peak appeared at 824 cm^{-1}, indicating that all double bonds converted to epoxide ring. The peak for the hydroxyl group appeared at 3466 cm^{-1} after reaction of ESO with RA and the peak for the epoxide group disappeared, indicating that all the epoxide rings reacted with RA to form SO−OH by ring opening. The intensity of hydroxyl peak is related to the number of double bonds. As the peak intensity for the double bond was low, the peak intensity of the corresponding hydroxyl groups was not so intense.

DOI: 10.1021/acssuschemeng.5b00001
ACS Sustainable Chem. Eng. XXXX, XXX, XXX−XXX

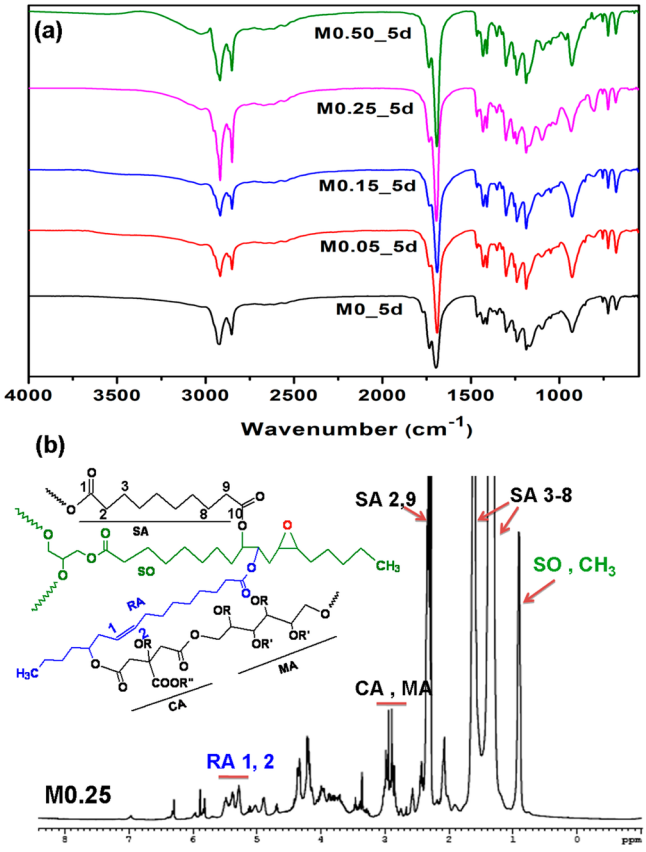

Figure 3. Chemical characterization of synthesized polyesters. FTIR spectra of M0, M0.05, M0.15, M0.25, and M0.50 after 5 days of postpolymerization (a) and ^{1}H NMR spectrum of purified M0.25 prepolymer (b).

Figure 2b shows the ^{1}H NMR spectra of SO, ESO, and SO−OH. The chemical shifts at 4.0−4.4 ppm and 5.3−5.5 ppm were attributed to the presence of glycerol backbone and unsaturated double bonds in SO. The peak for the methylene proton at the position 4 carbon atom (green) was obtained at 2.8 ppm. The peak intensity for the protons of unsaturated double bonds significantly decreased after epoxidation, and new peaks at 2.8−3.3 ppm appeared, indicating the formation of epoxide ring (indicated by 1, red) at the double bonds.[35] The chemical shifts at 1.5−2.2 also indicated the formation of epoxide ring at the double bonds. The peak intensity for epoxide ring decreased after reaction of ESO with RA and new peaks were observed at 4.9 ppm attributed to the proton attached to the newly formed ester bond (indicated by 2, blue).[36] Additionally, the peak for proton attached to the carbon adjacent to hydroxyl group was obtained at 3.5−3.8 ppm. The peak for unsaturated proton comes from RA and appeared at 5.3−5.6 ppm, indicating the chemical conjugation of RA with ESO to form SO−OH.

The synthesized SO−OH was reacted with SA and CA in the presence or absence of M. CA acts as a cross-linker with M as an additional reactant to yield a cross-linked polyester (Figure 1). The polyester was prepared by prepolymerization followed by postpolymerization. The prepolymers were synthesized by melt condensation followed by curing. Table 1 shows the different weight ratios of the monomers for the synthesis of the polyester with either CA or M. It was observed that the polymer of SO−OH:SA:CA:M with a weight ratio of 1:0.5:0.5:0 was elastomeric but soft after curing for 5 days.

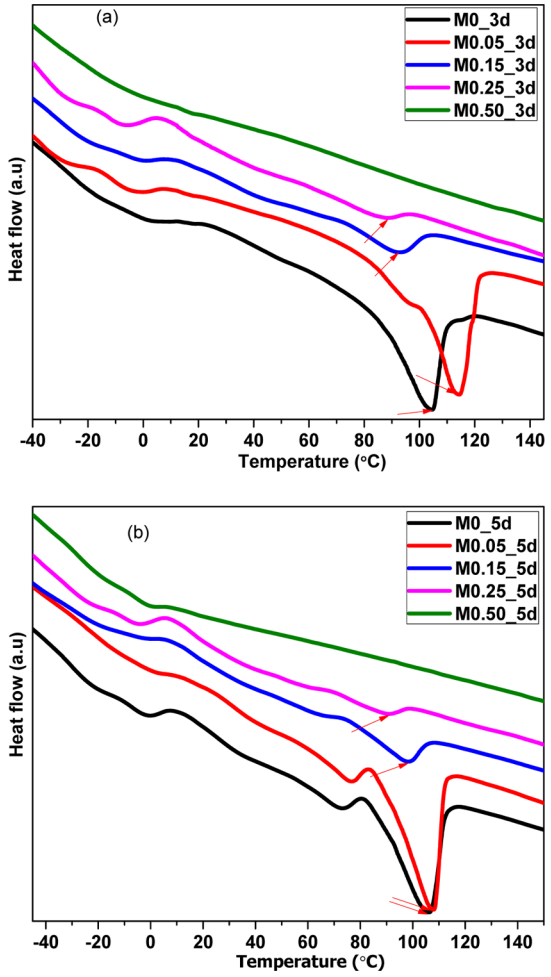

Figure 4. DSC of different polyesters with varying D-mannitol contents after 3 days (a) and 5 days (b) postpolymerization.

With an increase in CA content, the polymer was found to be brittle, and therefore, the cured polymer fragmented into smaller pieces when it was removed from the Petri dish after curing. Thus, M was added as an additional reactant (Table 2) to improve the mechanical properties of the polymer. However, the polyester prepared using only M in the absence of CA yielded a brittle polymer (Table 1). Thus, the polymers listed in Table 2 were used for further studies. The synthesized prepolymers were soluble in different solvents such as acetone, dioxane, THF, dimethyl sulfoxide (DMSO), and DMF, whereas postpolymerized polyesters were insoluble in the above solvents. All the prepolymers were analyzed using gel permeation chromatography to determine the molecular weights. All the prepolymers had molecular weights in the range of 1000−1200 Da. As the cured copolymers were not soluble in the solvents, the molecular weights of the cured copolyesters could not be determined. To determine the gel fraction of these polyesters after curing, the polymers were first swelled in DMSO for 24 h and then dried under vacuum for 24 h. The swelling ratio and the sol content were computed from the weight gain and weight loss, respectively and given in Table 2. It is clearly observed that the swelling ratio and % of sol content decreased with increasing M content or increased curing time.

Structural Characterization of Polyester. Figure 3a shows the FTIR spectra of the polyesters after 5 days

DOI: 10.1021/acssuschemeng.5b00001
ACS Sustainable Chem. Eng. XXXX, XXX, XXX−XXX

Table 3. Thermal Properties of the Copolyesters Cured for 3 and 5 Days

		thermal properties (±1 °C)					
		3 day cured			5 day cured		
code	weight ratio SO−OH:SA:CA:M	T_g (°C)	T_m (°C)	T_c (°C)	T_g (°C)	T_m (°C)	T_c (°C)
M0	1:0.5:0.5:0	−11	104	68	−7	106	69
M0.05	1:0.5:0.5:0.05	−11	114	84	−7	108	70
M0.15	1:0.5:0.5:0.15	−11	92	46	−7	98	48
M0.25	1:0.5:0.5:0.25	−12	87	26	−8	91	38
M0.50	1:0.5:0.5:0.5	−14	a[a]	a	−11	a	a

[a]The "a" indicates no T_m and T_c values were observed.

postpolymerization without M and varying amounts of M. The absorption peak for hydroxyl group at 3466 cm^{-1} presented in SO−OH disappeared after postpolymerization, indicating that all hydroxyl groups reacted with carboxylic acid groups of SA and CA to form ester bonds. The corresponding ester peak was obtained at 1696 cm^{-1} along with the triglyceride ester peak at 1736 cm^{-1}. The peak at 1736 cm^{-1} is ascribed to free ester (C═O stretching) bond, whereas the peak at 1696 cm^{-1} is due to hydrogen bonded C═O stretching after the curing process. Similar results were obtained when ESO in the presence of tetraethylammonium bromide catalyst was thermally cured by using methylhexahydrophthalic anhydride (curing agent).[37,38] The peak intensity of the ester bond gradually increased with increase in M content that can be attributed to the formation of more ester bonds. The peaks at 2922 and 2852 cm^{-1} arise due to the $-CH_2$ symmetrical and asymmetrical stretch, respectively. Figure S1 of the Supporting Information shows the FTIR spectra of M0 and M0.25 polyesters postpolymerized for 3 and 5 days. A broad peak of hydroxyl stretching at 3466 cm^{-1} was absent and C═O stretching of ester increased for both polyesters at 5 days postpolymerization compared 3 days, indicating the 5 days postpolymerization reached saturation of polymerization.

To confirm the observations in FTIR, ^1H and ^{13}C NMR were also carried out. Figure 3b shows the ^1H NMR spectra of purified prepolymer of M0.25. From proton NMR, it was not possible to determine the monomer composition in the prepolymer due to overlapping peaks. NMR confirmed the presence of all monomers in the polymer. The peaks at 5.3−5.8 ppm correspond to the protons attached to the unsaturated carbon atoms present in RA. SA showed the peaks at 1.2−1.8 and 2.4 ppm. The overlapped peak at 2.8−3.2 ppm was obtained for both CA and M. The alcohol peaks of M and CA overlap δ at 3.3 to 4 ppm.[33]

The synthesis of SO−OH and polyesters was further verified by ^{13}C NMR spectrum (Figure S2 of the Supporting Information). In SO, the chemical shifts were observed at 172.5 ppm and 128−130 ppm due to carbonyl carbon of triglyceride and unsaturated carbons, respectively. Other peaks at 22−34 ppm were related to methylene carbons, and the peak at 14 ppm corresponds to terminal carbon of methyl ($-CH_3$) groups.[39] After epoxidation of SO, a new peak appeared at 52 ppm, indicating the formation of the epoxide ring.[40]

The peak height at 52 ppm, corresponding to the carbon atoms of epoxide ring, is small in the ^{13}C NMR spectra. However, additional evidence is provided by FTIR and NMR. FTIR and ^1H NMR spectra showed strong peak at 824 cm^{-1} and 2.8−3.3 ppm, respectively, indicating and confirming the presence of epoxide ring in ESO.

The disappearance of peak at 52 ppm was due to reaction of ESO with RA.[40] The α, β, and the remaining methylene carbons of SA were observed around 24 to 36 ppm. The carboxylic carbon peaks for SA and CA were obtained at around 175 and 170 ppm. The quaternary carbon in CA in M0 is seen as the small peak at around 75 ppm.[41] For M0.25, the additional peaks for carbon atoms of M appeared within 62−65 ppm.[41]

Thermal Properties. Figure 4a,b shows the DSC thermograms of all the polymers cured for 3 and 5 days, respectively. Table 3 summarizes their glass transition (T_g), melting (T_m), and crystallization (T_c) temperature for the cured samples. Similarly, T_m and T_c peaks were observed in M0.05 and M0.25. It appears that, at low concentrations, M does not hinder the formation of crystalline phases, which is indicated by the T_m and T_c peaks. At a higher concentration of M (M0.50), no melting and crystallization peaks were observed and this suggests that M0.5 is amorphous. This is likely because a higher fraction of M added into polymer matrix leads to increased cross-linking of the polymer chains, which leads to a decrease in free volume and acts as an impediment in polymer crystallization.[42] The extremely large number ester and hydrogen bonds formed appears to have resulted in an amorphous M0.5 polyester.[43] All the compositions of polyester showed T_g values less than 0 °C, which indicates that the polyesters will exhibit nonglassy behavior in vivo (at 37 °C). As shown in Table 4, the cross-linking density increased, whereas molecular weight between cross-links (M_c) decreased with an increase in M content. The increased cross-linking density and shorter M_c imparts increased amorphous content consistent with the findings from DSC, as discussed above.

Mechanical Properties. For tissue engineering, the elastic modulus of these polymers is an important parameter, as they have to match the modulus of different tissues in the human body. Table 4 shows the percentage elongation at break, tensile strength, and elastic modulus determined from tensile stress−strain curves for all the polyesters of different M content after 3 and 5 days of curing. Representative stress−strain plots of all the polyesters after 3 and 5 days of curing are shown in Figure 5a,b, respectively. The elastic modulus gradually increased from 0.44 to 1.33 MPa with increase in M content in the polyester at 3 days. The elongation at break decreased monotonically from 107% to 18% with increase in M content. The modulus further increased (ranging from 0.46 to 3.17 MPa with increased M content) with increase in the curing time to 5 days. The elongation at break gradually decreased (ranging from 68% to 8% with increasing M content) for polyesters cured for 5 days. M0.5 after 5 days of curing was too brittle and lacked the elastomeric nature desired for preparing tissue scaffolds. These trends arise because of increase in extent of cross-linking with

DOI: 10.1021/acssuschemeng.5b00001
ACS Sustainable Chem. Eng. XXXX, XXX, XXX−XXX

Table 4. Physical and Mechanical Properties of the Copolyesters

	3 day cured						5 day cured					
	mechanical properties						mechanical properties					
sample code	elastic modulus (MPa)	tensile strength (MPa)	elongation (%)	cross-linking density n (mol/m^3)	molecular weight between cross-links M_c (g mol^{-1})	water contact angle (deg)	elastic modulus (MPa)	tensile strength (MPa)	elongation (%)	cross-linking density n (mol/m^3)	molecular weight between cross-links M_c (g mol^{-1})	water contact angle (deg)
M0	0.44 ± 0.05	0.77 ± 0.04	107 ± 10	58.8 ± 6.7	16010	83.4 ± 0.4	0.46 ± 0.14	0.14 ± 0.04	68 ± 12	61.5 ± 18.7	15314	86.1 ± 0.7
M0.05	0.54 ± 0.07	0.55 ± 0.05	86 ± 7	72.2 ± 9.4	14976	88.5 ± 2.6	0.93 ± 0.14	0.28 ± 0.19	63 ± 5	124.3 ± 18.6	11114	89.9 ± 2.3
M0.15	0.93 ± 0.16	0.49 ± 0.02	73 ± 2	124.3 ± 21.4	9563	93.3 ± 1.8	1.36 ± 0.22	0.31 ± 0.07	53 ± 9	208.5 ± 29.4	5702	96.3 ± 1.2
M0.25	1.02 ± 0.18	0.37 ± 0.12	43 ± 11	136.3 ± 24.1	8858	97.6 ± 2.6	1.97 ± 0.22	0.39 ± 0.11	22 ± 4	263.3 ± 29.4	4586	98.2 ± 2.7
M0.50	1.33 ± 0.19	0.11 ± 0.03	18 ± 7	177.7 ± 25.4	7340	96.5 ± 2.5	3.17 ± 0.12	0.30 ± 0.07	8 ± 4	423.6 ± 16.0	3079	98.3 ± 1.2

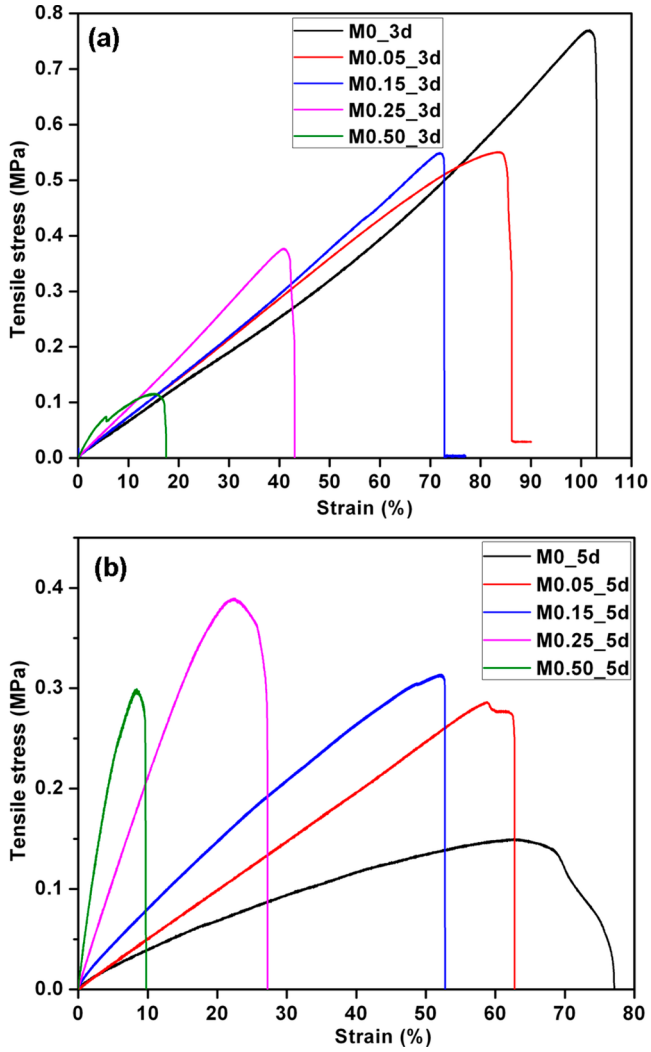

Figure 5. Representative stress−strain curves of different polyesters cured for (a) 3 days and (b) 5 days. All experiments are based on six experiments per sample.

increase in M content and/or curing time. This observation was validated from the cross-linking density measurement using rubber elasticity equation showing that the degree of cross-linking density gradually increased from M0 to M0.50 (Table 4).

The elastic modulus of these polymers closely matches that of human tissues such as human cervical spinal components, ligaments, and soft collagenous bone. The elastic modulus value of elastin from bovine ligament, ligamentum flavum, and interspinous ligaments were 1.1, 1.5, and 1.5 MPa, respectively.[44,45] Thus, these polymers could potentially be explored for use in different tissues in the human body. The elastomeric nature of these polyesters compare favorably with those of SO based polyurethanes reported previously for use as tissue scaffolds. A number of SO based polyurethanes have been reported and these tend to be chemically stable, and mechanically brittle and hard.[17,18,46] SO−OH was reacted with biobased oils to yield polyols, which were reacted with isocyanate to prepare polyurethanes.[47] The T_g of these polymers is significantly higher than 37 °C, such that they are nonelastomeric at physiological conditions. Thus, such polyurethanes are not well suited for tissue regeneration and drug delivery that require the use of biodegradable polymers. In

DOI: 10.1021/acssuschemeng.5b00001
ACS Sustainable Chem. Eng. XXXX, XXX, XXX−XXX

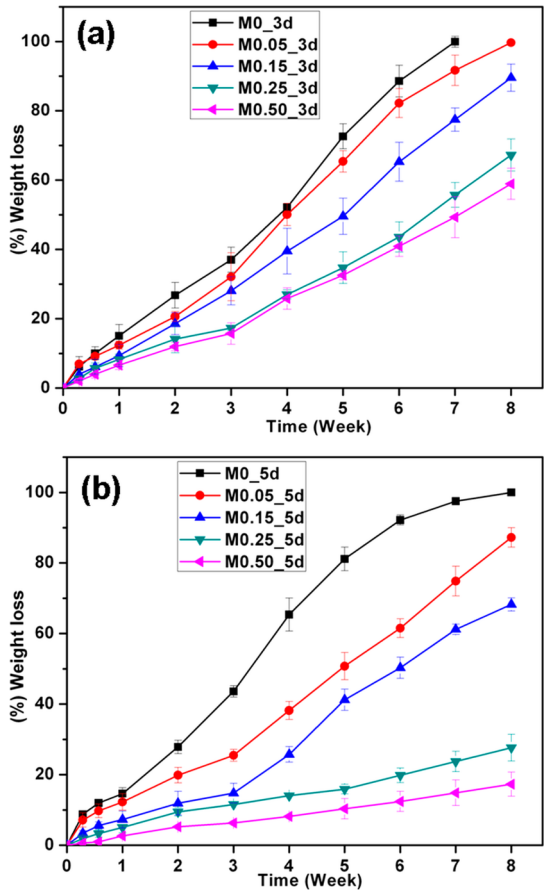

Figure 6. In vitro hydrolytic degradation profiles of 3 day (a) and 5 day (b) cured polyesters. All experiments were conducted in triplicate and the error bars represent one standard deviation.

Table 5. Degradation Rate Constant

	k_d (g h^{-1})	
polymer	3 day cured	5 day cured
M0	8.9	8.4
M0.05	6.4	5.1
M0.15	5.6	2.9
M0.25	3.4	2.3
M0.50	3.1	1.3

a recent study, a biodegradable phosphoester prepared from castor oil and SO has been reported and its use in biomedical applications has been proposed.[48]

Wettability Study. Surface water wettability of a polymer is important for its use as a biomaterial, as it determines its degradation rate, drug release kinetics, protein adsorption, and cellular response. Table 4 tabulates the water contact angles of polyesters cured for 3 and 5 days. The contact angle for 3 day cured polyesters was marginally lower than that of 5 day cured. This increase in water contact angle may be attributed to the reduced availability of unreacted hydroxyl functional groups with curing. The contact angle was approximately 85° for the 5 day cured M0 polymer. It gradually increased from 85° to 95° with increasing M content in the polymer. It was expected that the increase in M content in the polyester would afford more hydrophilic (OH) groups to the polymer surface and thereby increase the wettability. Interestingly, the polyester surface showed a decrease in wettability (higher contact angle) as the curing time and concentration of the M increased. This suggests that all the free hydroxyl groups likely reacted with carboxyl groups present in the other monomers, leading to the formation of long aliphatic carbon chains.

Degradation Study. Figure 6a,b shows the degradation profiles of polyesters cured for 3 and 5 days in PBS (pH 7.4) at 37 °C. Complete degradation (100% weight loss) of M0 polymer was observed after the seventh week (1176 h) for 3 day cured and eighth week (1344 h) for 5 day cured samples. Further, the degradation rate gradually decreased with increase in M content in the polyester. After 8 weeks, the weight loss of M0.05, M0.15, M0.25, and M0.50 was 99%, 89%, 67%, and 59% for 3 day cured, respectively, and 87%, 68% 28% and 17% for 5 day cured polymers, respectively. The degradation rate decreased around 40% for 3 day cured and 80% for 5 day cured M0.50 compared to the corresponding M0 samples by 8 weeks. The initial kinetics of degradation was modeled as zero-order rate law (where k_d is the rate constant of degradation) as follows

$$-\frac{dM_t}{dt} = k_d \tag{3a}$$

In eq 3a, M_0 is the initial mass and M_t is mass of polymer after degradation at a given time t. The equation may be solved to obtain

$$\frac{M_t}{M_0} = 1 - \frac{k_d}{M_0}t \tag{3b}$$

The values of k_d are compiled in Table 5 and are determined from the initial slopes of the lines in Figure 6a,b. These results indicate that k_d decreased with increase in cross-linking either due to prolonged curing or increased M content. This is due to the higher cross-linking density which can lead to the formation of longer hydrophobic polymer chains which lowers the diffusion coefficient and maximum resistance against hydrolysis. These data are also consistent with the hydrophobicity of the polymer (water contact angles in Table 4). Increased hydrophobicity tends to moderate hydrolytic degradation of the polyesters likely because of the ingress of the water into the polymer for hydrolytic degradation is retarded.

Dye Release. The release kinetics of the dyes, RB and RBB, from 3 and 5 day cured M0 and M0.25 polymers were investigated (Figure 7a,b) because these polymers exhibit markedly different mechanical properties and degradation profiles. After 720 h, the fractions of RB released from the 3 day cured M0 and M0.25 polymers were 99% and 55%, respectively. The corresponding values were 80% and 50% from the 5 day cured polyesters. In the case of RBB loaded M0 and M0.25, the fractions of dye released were 44% and 23% for 3 day cured polymers, respectively; and 39% and 19% for 5 day cured polyesters after 720 h. RB was released faster than RBB from the M0 in a controlled manner. A similar result was also observed for M0.25. This may be attributed to the presence of more hydrophilic tert N^+ group and Cl^- ions in RB relative to the more hydrophobic RBB dye. Hydrophobic interactions between a hydrophobic dye and the hydrophobic polyesters prepared in this study will moderate the release of RBB relative to RB. Interestingly, as the hydrophobicity of the polymer increased with increased cross-linking due to either increased curing time or M content, the release of RB and RBB from both MO and M0.25 polymers slowed. Because the dye release is determined by the hydrolytic degradation and erosion of the

DOI: 10.1021/acssuschemeng.5b00001
ACS Sustainable Chem. Eng. XXXX, XXX, XXX−XXX

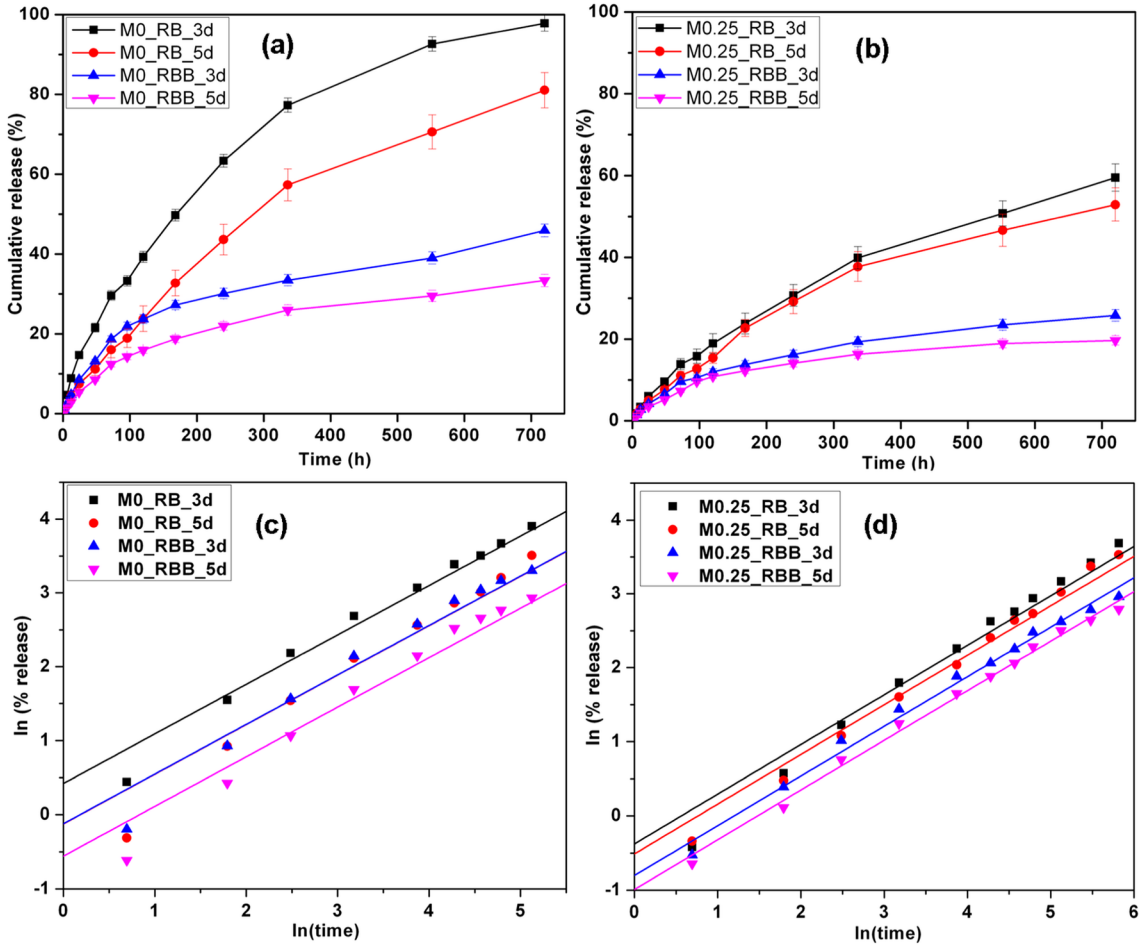

Figure 7. In vitro release profiles of model hydrophilic RB dye and model hydrophobic RBB dye from M0 (a) and M0.25 (b) polymers cured for 3 and 5 days. The error bars indicate standard deviation between three replicates. The log−log plots of (M_t/M_∞) versus time (based on eq 5) for M0 (c) and M0.25 (d) of RB and RBB release. All experiments were conducted in triplicate and the error bars represent one standard deviation.

Table 6. Dye Release Rate Constant

	M0_RB		M0_RBB		M0.25_RB		M0.25_RBB	
rate constant	3 days	5 days	3 days	5 days	3 days	5 days	3 days	5 days
k (h^{-n})	1.5	0.9	0.9	0.6	0.7	0.6	0.5	0.4

polymer, increased hydrophobhicity resulting from increased cross-linking retarded the dye release. We recently observed similar trends of dye loaded hydrophobic poly(xylitol dicarboxylate) polyesters.[49]

The dye release mechanism can be modeled using the Korsmeyer−Peppas semiempirical relation[50] to determine the dye dissolution profile

$$\frac{M_t}{M_\infty} = kt^n \tag{4}$$

where M_t is the dye released at time t, M_∞ is the total amount of dye released, k is the rate constant, and n is the release exponent. Equation 4 can be written as

$$\ln\left(\frac{M_t}{M_\infty}\right) = \ln(k) + n\ln t \tag{5}$$

Figure 7c,d shows that log−log plots of (M_t/M_∞) versus time of RB and RBB released are linear for both M0 and M0.25 polyesters. A value of $n = 0.67$ was used to fit the data for the initial release. A value of $n > 0.5$ indicates the polyesters exhibit a non-Fickian/anomalous release behavior.[50] The values of the parameter k were calculated from the RB and RBB release profiles, and are tabulated in Table 6. The k value of RB was lower than the corresponding value for RBB for a given polymer. The value decreased for both RB and RBB with increased curing time. The value also decreased with increased M content. The release of the dye is governed by a number of factors such as uniform dispersion of drug in polymer matrix, solubility of the drug in dispersion media, bonding between drug and polymer, polymer hydrolytic degradation, degree of cross-linking, porosity, size of drug molecules, and wettability.[51] The observation that k decreased for RB and RBB as M content increased or curing time increased suggests that the release depends on the degree of cross-linking between polymer chains and, as a result, on the degradation rate of polymer and its water contact angle. M0.25 could thus be used for sustained drug delivery system, whereas M0 can be used for the rapid release of a drug. In tissue engineering, drugs and biomolecules are commonly released from the scaffolds. Rapid release of antimicrobial and anti-inflammatory drugs at the implantation site may be desired for certain applications, whereas sustained release of osteoinductive factors can be leveraged to stimulate stem and progenitor cells to augment tissue formation in the case of bone regeneration, for example.

DOI: 10.1021/acssuschemeng.5b00001
ACS Sustainable Chem. Eng. XXXX, XXX, XXX−XXX

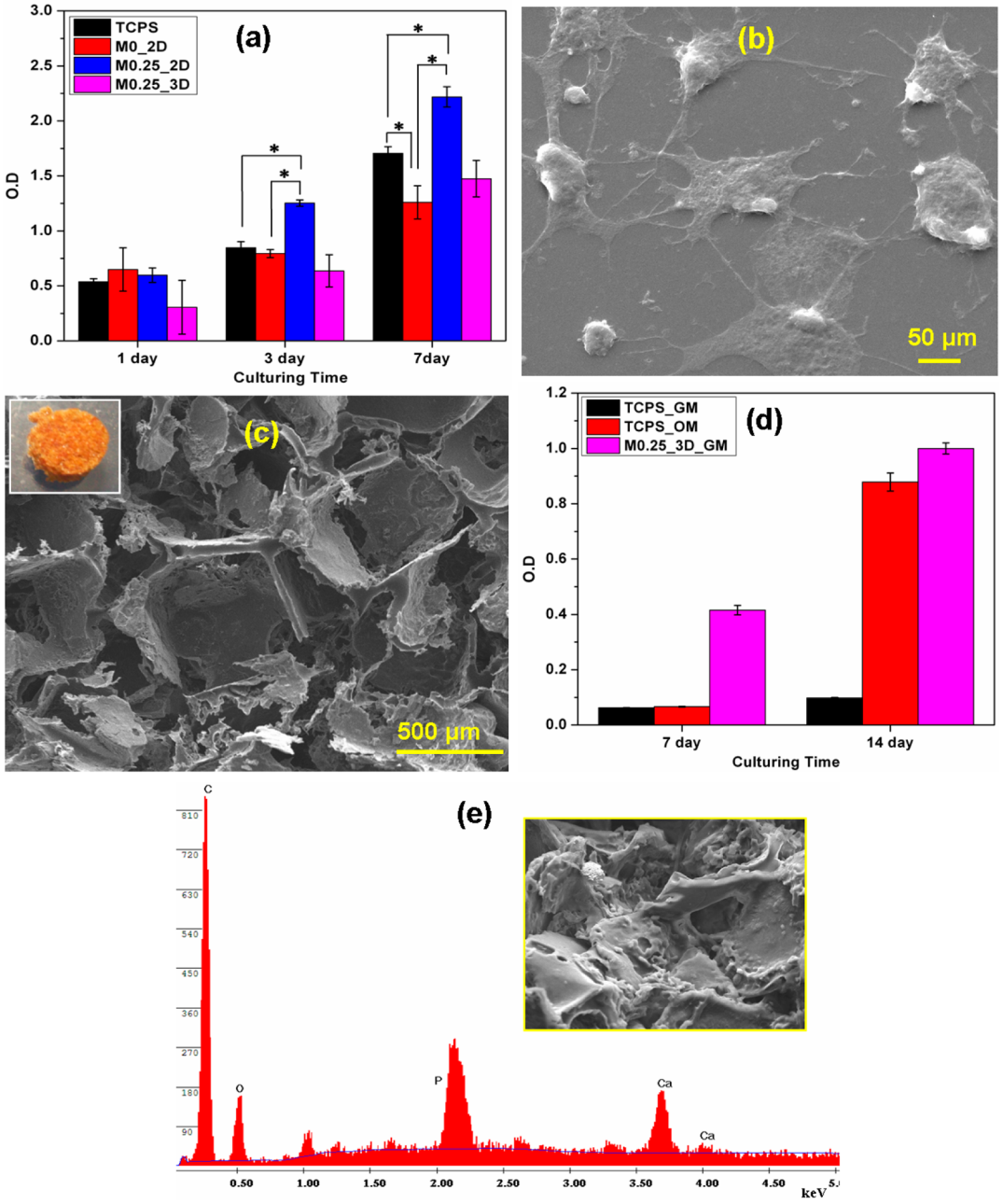

Figure 8. Stem cell response to the polymer. hMSC proliferation in growth medium (GM) on tissue culture polystyrene (TCPS) surface, M0_2D and M0.25_2D films, and M0.25_3D scaffold measured using WST assay at 1, 3, and 7 days (a); SEM micrograph of cells on M0.25_2D film at day 3 (b); SEM micrograph of porous M0.25_3D scaffold with inset showing digital photograph of the whole scaffold (c); quantification of mineral deposition in M0.25_3D scaffold in GM, and on TCPS plates in GM and osteogenic medium (OM) by Alizarin red assay at 7 and 14 days (d); SEM-EDX spectra confirming deposition of calcium phosphate minerals in M0.25_3D scaffold at day 14 with SEM of mineralized scaffold shown in the inset (e). Statistical analysis are based on assay data from six replicates each and an asterisk (*) indicates statistical significance ($p < 0.05$).

Cytocompatibility and Stem Cell Osteogenesis. The physicochemical characterization reported above showed that the polyesters prepared from ESO, CA, and SA optionally containing varying M content, as listed in Table 2, exhibited elastomeric properties and were thus potential candidates for preparing tissue scaffolds. Increasing M content up to 0.25 improved mechanical properties and attenuated the rate of hydrolytic degradation. The polyester was brittle and non-elastomeric with a low % elongation at break at higher M content (M0.5). It was also observed that the porous scaffolds could not be prepared from M0.5, as further discussed below. Thus, films of M0 and M0.25 cured for 5 days prepared by drop casting were used to evaluate cytocompatibility in 2D culture format (cells on surface). Primary bone marrow hMSCs were used for this work, as the polymer is intended for use in tissue regeneration. hMSCs are multipotential cells that are being widely studied for use in stem cell based therapies. Osteogenic differentiation of hMSCs is well established. Cells on the films and scaffold were evaluated using the WST assay, which measures mitochondrial activity of viable cells, and is thus taken as a measure of the number of cells at 1, 3, and 7 days (Figure 8a). There were no significant differences between the numbers of attached cells at 1 day. The increase in optical density (O.D.) at days 3 and 7 suggests an increase in number of cells. At day

DOI: 10.1021/acssuschemeng.5b00001
ACS Sustainable Chem. Eng. XXXX, XXX, XXX−XXX

3, the number of cells was significantly higher on M0.25 than on M0 and TCPS.

At day 7, the number of cells was higher on M0.25 than TCPS, which was higher than on M0. Cell morphology was assessed by SEM. Figure 8b is the representative micrograph of cells on M0.25 at 3 days. hMSCs are conventionally known to exhibit an elongated, spindle-shaped morphology on TCPS surfaces. In contrast, we observed that the cells exhibited a less spread, rounded morphology on these polymers, likely due to the hydrophobic nature of the polymers. Thus, both polymers M0 and M0.25 were determined to be cytocompatible and capable of supporting cell proliferation.

Macroporous scaffolds are widely prepared for tissue engineering, and salt leaching is the most commonly used technique wherein sodium chloride is used as the porogen. 250−425 μm sized salt crystals were used, as this range is postulated to be optimal for bone tissue engineering.[52] Scaffolds were prepared using M0.25, as it was observed to be better in supporting cell growth, as discussed above. SEM micrographs revealed an interconnected open porous structure of the scaffolds with pores in the size range of approximately 240−400 μm (Figure 8c).

Osteogenic differentiation of hMSCs in M0.25 scaffolds was confirmed by formation of mineral deposits at 7 days that significantly increased by day 14, as revealed by ARS quantification (Figure 8d). Little mineralization could be seen on TCPS surfaces in OM at 7 and 14 days, as expected. In OM, mineralization on TCPS at 14 days was comparable to that in the scaffolds. Note that in vitro mineralization of hMSCs in the scaffolds was observed in the scaffolds even in the absence of soluble osteoinductive factors. The chemical nature of the mineral deposits was confirmed from SEM-EDX, which indicated characteristic P and Ca peaks (Figure 8e) corroborating the findings of the ARS results. CA is an important component of bone and has been implicated in mineralization.[53] The presence of CA in the polymer and its putative release after degradation of the polymer could have played an important role in driving osteogenesis, as is reported recently.[54] The role, if any, of the other polymer degradation products on driving stem cell fate is less well understood and will require further investigation. Thus, the M0.25 scaffold was found to induce hMSC osteogensis, leading to formation of calcium phosphate deposits in the scaffolds, suggesting that these polymers could be used in bone tissue engineering.

CONCLUSION

A family of biocompatible, biodegradable copolyesters based on SO along with other monomers from abundantly available, inexpensive, renewable resources such as SA, CA, and M was prepared by melt condensation. The polymers were elastomeric at physiological temperature. The mechanical properties and degradation rate of the polyester can be tuned by varying the monomer compositions and curing time. Attachment and proliferation of hMSCs in vitro confirmed that the polymers were cytocompatible. A 3D porous scaffold induced osteogenesis of hMSCs even in the absence of osteoinductive factors, suggesting its use in bone tissue engineering. This family of copolyesters offers low cost, green, biocompatible, bioresorbable polymers for potential use as resorbable biomaterials. The physicochemical properties of these polymers can be tailored for tissue-specific applications including both tissue regeneration and controlled release by varying the composition and curing time.

ASSOCIATED CONTENT

Supporting Information

FTIR spectra of M0 and M0.25 polyester at two different postpolymerization times of 3 and 5 days (Figure S1); ^{13}C NMR spectra of SO, ESO, SO−OH, and M0.25 prepolymer (Figure S2a−d). This material is available free of charge via the Internet at http://pubs.acs.org/.

AUTHOR INFORMATION

Corresponding Author

*K. Chatterjee. E-mail: kchatterjee@materials.iisc.ernet.in.

Notes

The authors declare no competing financial interest.

ACKNOWLEDGMENTS

This work was funded by the Department of Biotechnology (DBT), India. K.E. gratefully acknowledges DBT for the Postdoctoral Research Associate Fellowship. K.S. was supported by the D.S. Kothari Fellowship from the University Grants Commission (UGC), India. K.C. acknowledges Ramanujan fellowship from the Department of Science and Technology (DST), India.

REFERENCES

(1) O'Brien, F. J. Biomaterials & scaffolds for tissue engineering. *Mater. Today* **2011**, *14* (3), 88−95.
(2) Langer, R. Biomaterials in drug delivery and tissue engineering: One laboratory's experience. *Acc. Chem. Res.* **2000**, *33* (2), 94−101.
(3) Bose, S.; Vahabzadeh, S.; Bandyopadhyay, A. Bone tissue engineering using 3D printing. *Mater. Today* **2013**, *16* (12), 496−504.
(4) Gunatillake, P. A.; Adhikari, R. Biodegradable synthetic polymers for tissue engineering. *Eur. Cell. Mater.* **2003**, *5* (1), 1−16.
(5) Cheung, R. Y.; Ying, Y.; Rauth, A. M.; Marcon, N.; Yu Wu, X. Biodegradable dextran-based microspheres for delivery of anticancer drug mitomycin C. *Biomaterials* **2005**, *26* (26), 5375−5385.
(6) Ulery, B. D.; Nair, L. S.; Laurencin, C. T. Biomedical applications of biodegradable polymers. *J. Polym. Sci., Part B: Polym. Phys.* **2011**, *49* (12), 832−864.
(7) Natarajan, J.; Rattan, S.; Singh, U.; Madras, G.; Chatterjee, K. Polyanhydrides of castor oil−sebacic acid for controlled release applications. *Ind. Eng. Chem. Res.* **2014**, *53* (19), 7891−7901.
(8) Heller, J.; Barr, J.; Ng, S. Y.; Abdellauoi, K. S.; Gurny, R. Poly(ortho esters): Synthesis, characterization, properties and uses. *Adv. Drug Delivery. Rev.* **2002**, *54* (7), 1015−1039.
(9) Laurencin, C. T.; Norman, M. E.; Elgendy, H. M.; el-Amin, S. F.; Allcock, H. R.; Pucher, S. R.; Ambrosio, A. A. Use of polyphosphazenes for skeletal tissue regeneration. *J. Biomed. Mater. Res.* **1993**, *27* (7), 963−973.
(10) Chanprateep, S. Current trends in biodegradable polyhydroxyalkanoates. *J. Biosci. Bioeng.* **2010**, *110* (6), 621−632.
(11) Dunkelman, N. S.; Zimber, M. P.; LeBaron, R. G.; Pavelec, R.; Kwan, M.; Purchio, A. Cartilage production by rabbit articular chondrocytes on polyglycolic acid scaffolds in a closed bioreactor system. *Biotechnol. Bioeng.* **1995**, *46* (4), 299−305.
(12) Jonoobi, M.; Mathew, A. P.; Abdi, M. M.; Makinejad, M. D.; Oksman, K. A comparison of modified and unmodified cellulose nanofiber reinforced polylactic acid (PLA) prepared by twin screw extrusion. *J. Polym. Environ.* **2012**, *20* (4), 991−997.
(13) Lu, T.-L.; Sun, W.-g.; Zhao, W.; Chen, T. Preparation of amifostine polylactide-co-glycolide microspheres and its irradiation protective to mouse through oral administration. *Drug Dev. Ind. Pharm.* **2011**, *37* (12), 1473−1480.
(14) Daebritz, S. H.; Fausten, B.; Hermanns, B.; Schroeder, J.; Groetzner, J.; Autschbach, R.; Messmer, B. J.; Sachweh, J. S. Introduction of a flexible polymeric heart valve prosthesis with special

DOI: 10.1021/acssuschemeng.5b00001
ACS Sustainable Chem. Eng. XXXX, XXX, XXX−XXX

design for aortic position. *Eur. J. Cardiothorac. Surg.* **2004**, *25* (6), 946−952.
(15) Barrett, D. G.; Yousaf, M. N. Design and applications of biodegradable polyester tissue scaffolds based on endogenous monomers found in human metabolism. *Molecules* **2009**, *14* (10), 4022−4050.
(16) Miao, S.; Wang, P.; Su, Z.; Zhang, S. Vegetable-oil-based polymers as future polymeric biomaterials. *Acta Biomater.* **2014**, *10* (4), 1692−1704.
(17) Tan, S.; Abraham, T.; Ference, D.; Macosko, C. W. Rigid polyurethane foams from a soybean oil-based polyol. *Polymer* **2011**, *52* (13), 2840−2846.
(18) Bahr, M.; Mulhaupt, R. Linseed and soybean oil-based polyurethanes prepared via the non-isocyanate route and catalytic carbon dioxide conversion. *Green Chem.* **2012**, *14* (2), 483−489.
(19) Howard, G. T. Biodegradation of polyurethane: A review. *Int. Biodeterior. Biodegrad.* **2002**, *49* (4), 245−252.
(20) Miao, S.; Sun, L.; Wang, P.; Liu, R.; Su, Z.; Zhang, S. Soybean oil-based polyurethane networks as candidate biomaterials: Synthesis and biocompatibility. *Eur. J. Lipid Sci. Technol.* **2012**, *114* (10), 1165−1174.
(21) Tokiwa, Y.; Calabia, B.; Ugwu, C.; Aiba, S. Biodegradability of Plastics. *Int. J. Mol. Sci.* **2009**, *10* (9), 3722−3742.
(22) Qin, Y.; Jia, J. R.; Zhao, L.; Huang, Z. X.; Zhao, S. W.; Zhang, G. W.; Dai, B. F. Synthesis and characterization of soybean oil based unsaturated polyester resin. *Adv. Mater. Res.* **2012**, *393*, 349−353.
(23) Dai, J.; Ma, S.; Han, L.; Zhang, L. Polyesters derived from itaconic acid for the properties and bio-based content enhancement of soybean oil-based thermosets. *Green Chem.* **2015**, DOI: 10.1039/C4GC02057J.
(24) Miyagawa, H.; Mohanty, A. K.; Burgueño, R.; Drzal, L. T.; Misra, M. Novel biobased resins from blends of functionalized soybean oil and unsaturated polyester resin. *J. Polym. Sci., Part B: Polym. Phys.* **2007**, *45* (6), 698−704.
(25) List, G.; Neff, W.; Holliday, R.; King, J.; Holser, R. Hydrogenation of soybean oil triglycerides: Effect of pressure on selectivity. *J. Am. Oil Chem. Soc.* **2000**, *77* (3), 311−314.
(26) Zhang, C.; Xia, Y.; Chen, R.; Huh, S.; Johnston, P. A.; Kessler, M. R. Soy-castor oil based polyols prepared using a solvent-free and catalyst-free method and polyurethanes therefrom. *Green Chem.* **2013**, *15* (6), 1477−1484.
(27) Krasko, M. Y.; Shikanov, A.; Ezra, A.; Domb, A. J. Poly(ester anhydride)s prepared by the insertion of ricinoleic acid into poly(sebacic acid). *J. Polym. Sci., Part A: Polym. Chem.* **2003**, *41* (8), 1059−1069.
(28) Vieira, C.; Evangelista, S.; Cirillo, R.; Lippi, A.; Maggi, C. A.; Manzini, S. Effect of ricinoleic acid in acute and subchronic experimental models of inflammation. *Mediators Inflamm.* **2000**, *9* (5), 223−228.
(29) Chandorkar, Y.; Madras, G.; Basu, B. Structure, tensile properties and cytotoxicity assessment of sebacic acid based biodegradable polyesters with ricinoleic acid. *J. Mater. Chem.* **2013**, *1* (6), 865−875.
(30) Yang, J.; Webb, A. R.; Ameer, G. A. Novel citric acid-based biodegradable elastomers for tissue engineering. *Adv. Mater.* **2004**, *16* (6), 511−516.
(31) Katti, D.; Lakshmi, S.; Langer, R.; Laurencin, C. Toxicity, biodegradation and elimination of polyanhydrides. *Adv. Drug Delivery. Rev.* **2002**, *54* (7), 933−961.
(32) Saithai, P.; Lecomte, J.; Dubreucq, E.; Tanrattanakul, V. Effects of different epoxidation methods of soybean oil on the characteristics of acrylated epoxidized soybean oil-co-poly(methyl methacrylate) copolymer. *eXPRESS Polym. Lett.* **2013**, *7* (11), 910−924.
(33) Sarkar, K.; Krishna Meka, S. R.; Bagchi, A.; Krishna, N. S.; Ramachandra, S. G.; Madras, G.; Chatterjee, K. Polyester derived from recycled poly(ethylene terephthalate) waste for regenerative medicine. *RSC Adv.* **2014**, *4* (102), 58805−58815.
(34) Kumar, S.; Raj, S.; Kolanthai, E.; Sood, A. K.; Sampath, S.; Chatterjee, K. Chemical functionalization of graphene to augment stem cell osteogenesis and inhibit biofilm formation on polymer composites for orthopedic applications. *ACS Appl. Mater. Interfaces* **2015**, *7* (5), 3237−3252.
(35) Lu, Y.; Larock, R. C. New hybrid latexes from a soybean oil-based waterborne polyurethane and acrylics via emulsion polymerization. *Biomacromolecules* **2007**, *8* (10), 3108−3114.
(36) Xia, Y.; Larock, R. C. Castor oil-based thermosets with varied crosslink densities prepared by ring-opening metathesis polymerization (ROMP). *Polymer* **2010**, *51* (12), 2508−2514.
(37) Tan, S.; Chow, W. Thermal properties, curing characteristics and water absorption of soybean oil-based thermoset. *eXPRESS Polym. Lett.* **2011**, *5* (6), 480−492.
(38) Lu, Y.; Larock, R. C. Soybean-oil-based waterborne polyurethane dispersions: Effects of polyol functionality and hard segment content on properties. *Biomacromolecules* **2008**, *9* (11), 3332−3340.
(39) Zhang, P.; Zhang, J. One-step acrylation of soybean oil (SO) for the preparation of SO-based macromonomers. *Green Chem.* **2013**, *15* (3), 641−645.
(40) Biswas, A.; Sharma, B. K.; Willett, J.; Advaryu, A.; Erhan, S.; Cheng, H. Azide derivatives of soybean oil and fatty esters. *J. Agric. Food Chem.* **2008**, *56* (14), 5611−5616.
(41) Sathiskumar, P.; Madras, G. Synthesis, characterization, degradation of biodegradable castor oil based polyesters. *Polym. Degrad. Stab.* **2011**, *96* (9), 1695−1704.
(42) Lei, L.; Ding, T.; Shi, R.; Liu, Q.; Zhang, L.; Chen, D.; Tian, W. Synthesis, characterization and in vitro degradation of a novel degradable poly((1,2-propanediol-sebacate)-citrate) bioelastomer. *Polym. Degrad. Stab.* **2007**, *92* (3), 389−396.
(43) Sharma, V. K.; Kalonia, D. S. Effect of vacuum drying on protein-mannitol interactions: The physical state of mannitol and protein structure in the dried state. *AAPS PharmSciTech* **2004**, *5* (1), 58−69.
(44) Ha, S. K. Finite element modeling of multi-level cervical spinal segments (C3−C6) and biomechanical analysis of an elastomer-type prosthetic disc. *Med. Eng. Phys.* **2006**, *28* (6), 534−541.
(45) Gosline, J.; Lillie, M.; Carrington, E.; Guerette, P.; Ortlepp, C.; Savage, K. Elastic proteins: biological roles and mechanical properties. *Philos. Trans. R. Soc., B* **2002**, *357* (1418), 121−132.
(46) Pan, X.; Sengupta, P.; Webster, D. C. High biobased content epoxy−anhydride thermosets from epoxidized sucrose esters of fatty acids. *Biomacromolecules* **2011**, *12* (6), 2416−2428.
(47) Caillol, S.; Desroches, M.; Boutevin, G.; Loubat, C.; Auvergne, R.; Boutevin, B. Synthesis of new polyester polyols from epoxidized vegetable oils and biobased acids. *Eur. J. Lipid Sci. Technol.* **2012**, *114* (12), 1447−1459.
(48) Liu, Z.; Xu, Y.; Cao, L.; Bao, C.; Sun, H.; Wang, L.; Dai, K.; Zhu, L. Phosphoester cross-linked vegetable oil to construct a biodegradable and biocompatible elastomer. *Soft Matter* **2012**, *8* (21), 5888−5895.
(49) Dasgupta, Q.; Chatterjee, K.; Madras, G. Combinatorial approach to develop tailored biodegradable poly(xylitol dicarboxylate) polyesters. *Biomacromolecules* **2014**, *15* (11), 4302−4313.
(50) Costa, P.; Sousa Lobo, J. M. Modeling and comparison of dissolution profiles. *Eur. J. Pharm. Sci.* **2001**, *13* (2), 123−133.
(51) Soppirnath, K. S.; Aminabhavi, T. M. Water transport and drug release study from cross-linked polyacrylamide grafted guar gum hydrogel microspheres for the controlled release application. *Eur. J. Pharm. Biopharm.* **2002**, *53* (1), 87−98.
(52) Murphy, C. M.; Haugh, M. G.; O'Brien, F. J. The effect of mean pore size on cell attachment, proliferation and migration in collagen−glycosaminoglycan scaffolds for bone tissue engineering. *Biomaterials* **2010**, *31* (3), 461−466.
(53) Hartles, R. Citrate in mineralized tissues. *Adv. Oral Biol.* **1964**, *1*, 225−253.
(54) Tran, R. T.; Wang, L.; Zhang, C.; Huang, M.; Tang, W.; Zhang, C.; Zhang, Z.; Jin, D.; Banik, B.; Brown, J. L.; Xie, Z.; Bai, X.; Yang, J. Synthesis and characterization of biomimetic citrate-based biodegradable composites. *J. Biomed. Mater. Res., Part A* **2014**, *102* (8), 2521−2532.

DOI: 10.1021/acssuschemeng.5b00001
ACS Sustainable Chem. Eng. XXXX, XXX, XXX−XXX